

PnPSelect: Plug-and-play IoT Device Selection Using Ultra-wideband Signals

ZHAOXIN CHANG, Institut Polytechnique de Paris, France

FUSANG ZHANG, Beihang University and Institute of Software, Chinese Academy of Sciences, China

JIE XIONG, Nanyang Technological University, Singapore

ZIYU LI, Institut Polytechnique de Paris, France

BADII JOUABER, Institut Polytechnique de Paris, France

DAQING ZHANG, Institut Polytechnique de Paris, France and Peking University, China

In recent years, the number of Internet of Things (IoT) devices in smart homes has rapidly increased. A key challenge affecting user experience is how to enable users to efficiently and intuitively select the devices they wish to control. This paper proposes PnPSelect, a plug-and-play IoT device selection solution utilizing Ultra-wideband (UWB) technology on commercial devices. Unlike previous works, PnPSelect does not require the installation of dedicated hardware on each IoT device, thereby reducing deployment costs and complexities, and achieving true plug-and-play functionality. To enable intuitive device selection, we introduce a pointing direction estimation method that utilizes UWB readings from a single anchor to infer the user's pointing direction. Additionally, we propose a lightweight device localization method that allows users to register new IoT devices by simply pointing at them from two distinct positions, eliminating the need for manual measurements. We implement PnPSelect on commercial smartphones and smartwatches and conduct extensive evaluations in both controlled laboratory settings and real-world environments. Our results demonstrate high accuracy, robustness, and adaptability, making PnPSelect a practical and scalable solution for next-generation smart home interactions.

CCS Concepts: • **Human-centered computing** → *Ubiquitous and mobile computing systems and tools*.

Additional Key Words and Phrases: IoT, Ultra-wideband, Device selection, Smart home

ACM Reference Format:

Zhaoxin Chang, Fusang Zhang, Jie Xiong, Ziyu Li, Badii Jouaber, and Daqing Zhang. 2025. PnPSelect: Plug-and-play IoT Device Selection Using Ultra-wideband Signals. 1, 1 (November 2025), 23 pages. <https://doi.org/10.1145/nnnnnnnn.nnnnnnnn>

1 Introduction

With the rapid advancement of IoT technology, an increasing number of devices can now be connected to the Internet. A prominent example is smart home appliances, such as lights, air conditioners, and TVs, which enable remote control and automation. This trend has revolutionized how we interact with our surroundings, enhancing convenience, comfort, and

This work is supported by the European Union through the Horizon EIC pathfinder challenge project SUSTAIN (No. 101071179) and the Innovative Medicines Initiative 2 Joint Undertaking project IDEA-FAST (No. 853981).

Authors' Contact Information: Zhaoxin Chang, Institut Polytechnique de Paris, SAMOVAR, Telecom SudParis, Palaiseau, France, zhaoxin.chang@telecom-sudparis.eu; Fusang Zhang, Beihang University and Institute of Software, Chinese Academy of Sciences, Beijing, China, fusang@iscas.ac.cn; Jie Xiong, Nanyang Technological University, Singapore, Singapore, jie.xiong@ntu.edu.sg; Ziyu Li, Institut Polytechnique de Paris, Palaiseau, France, liziyu0104@gmail.com; Badii Jouaber, Institut Polytechnique de Paris, SAMOVAR, Telecom SudParis, Palaiseau, France, badii.jouaber@telecom-sudparis.eu; Daqing Zhang, Institut Polytechnique de Paris, SAMOVAR, Telecom SudParis, Palaiseau, France and Peking University, Beijing, China, daqing.zhang@telecom-sudparis.eu.

Permission to make digital or hard copies of all or part of this work for personal or classroom use is granted without fee provided that copies are not made or distributed for profit or commercial advantage and that copies bear this notice and the full citation on the first page. Copyrights for components of this work owned by others than the author(s) must be honored. Abstracting with credit is permitted. To copy otherwise, or republish, to post on servers or to redistribute to lists, requires prior specific permission and/or a fee. Request permissions from permissions@acm.org.

© 2025 Copyright held by the owner/author(s). Publication rights licensed to ACM.

Manuscript submitted to ACM

efficiency in daily life. Unlike traditional devices that are typically controlled individually (e.g., through remote controls and switches), IoT devices within the same environment can be managed through a unified user interface. Currently, in many smart home environments, smartphones or voice assistants serve as primary interfaces for controlling IoT devices. For instance, users often select devices from a list displayed on a smartphone. However, this method can be time-consuming and inconvenient, particularly as the number of smart devices increases and similar devices (e.g., multiple lamps in the same room) become more common. On the other hand, voice assistant-based solutions offer convenience but face challenges such as limited working range, disruption in quiet environments, and susceptibility to noise interference.

Recent research has explored alternative interaction methods that utilize common household devices, such as smartphones, smartwatches, and earphones. These methods allow users to select an IoT device by looking at or pointing toward it, offering a more intuitive and user-friendly experience. Several solutions [16, 19, 30, 33] leverage smartphone cameras for IoT device selection, using computer vision (CV) algorithms to recognize objects in the device's field of view (FoV). However, camera-based methods may struggle in low-light conditions and are limited to recognizing devices present in predefined training datasets. Moreover, distinguishing between devices of the same type (e.g., two identical lamps in different locations) remains challenging for deep-learning-based CV algorithms [35].

The latest research took a different route by leveraging information from wireless signals for IoT device selection. The key insight behind wireless signal-based solutions is that, by installing dedicated wireless modules on each IoT device, a wireless channel can be established between the user device and IoT devices. The device being pointed at or looked at can then be determined by extracting signal features such as Time-of-Flight (ToF) and Angle-of-Arrival (AoA). For example, ToF estimation allows the system to measure distance variations between the user device and IoT devices during a pointing gesture. The device that exhibits the most significant distance change is likely the one being pointed at (Figure 2a). Similarly, AoA measurements help determine the direction of IoT devices relative to the orientation of the user device, allowing the system to identify the selected device based on which AoA value is closest to zero (Figure 2b). Unlike camera-based approaches, wireless signal-based solutions maintain high accuracy regardless of lighting conditions. Additionally, similar devices can be distinguished more easily because each IoT device maintains a unique wireless channel with the user device. Moreover, the computational complexity of signal processing is lower than that of image processing. Various wireless technologies, including UWB [12], acoustic signals [40], and Bluetooth [47], have been explored for this purpose. While promising, a significant limitation of existing wireless signal-based solutions is the requirement that each IoT device be equipped with a dedicated wireless module, such as a UWB transceiver or a Bluetooth module. However, most smart home appliances do not currently include UWB transceivers, and Bluetooth-based solutions require compatibility with specific Bluetooth protocols (e.g., Bluetooth 5.1), which limits applicability. Therefore, the requirement for each IoT device to be equipped with dedicated hardware presents a major barrier to achieving a true plug-and-play solution for real-world deployments.

In this paper, we propose PnPSelect, an IoT device selection solution that addresses this limitation, bringing wireless signal-based systems one step closer to real-world deployment. Specifically, we ask a question: ***Can the selection of a large number of IoT devices be achieved with a single dedicated wireless device?*** Figure 1 illustrates the envisioned application scenario. The user can simply point at the IoT device they wish to control using their device (e.g., a smartphone). By analyzing the connection between the user device and a single wireless device, the pointing direction of the user can be estimated for selecting a specific IoT device. Compared to existing solutions, this approach significantly reduces deployment costs and complexity. To realize this vision, the first step is to determine the most suitable wireless signal for device selection. While various wireless technologies (Wi-Fi, Bluetooth, 4G/5G, and UWB) are

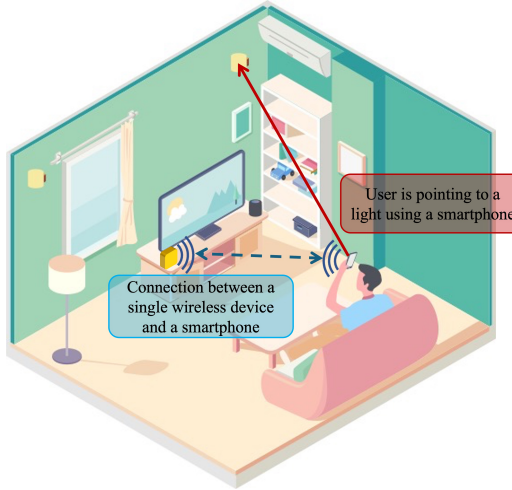


Fig. 1. The envisioned IoT device selection application scenario.

available on commodity devices, most are primarily designed for communication purposes. In contrast, UWB technology is inherently designed for precise ranging, and using it for device selection does not interfere with its original function. Notably, UWB modules are now integrated into a wide range of consumer devices, including those from Apple, Google, Huawei, Samsung, and Xiaomi. Therefore, we choose to utilize UWB signals available on commercial devices for IoT device selection.

Achieving IoT device selection with a single UWB device in the environment presents several challenges. The first one is estimating the pointing direction of the user device. Since IoT devices are not equipped with UWB transceivers, the user device lacks a direct connection to them and cannot rely on conventional ToF or AoA measurements. Instead, we leverage a key observation: when a user performs a pointing gesture, UWB signals can be used to track the movement of their device. By analyzing the trajectory of this movement, we can infer the pointing direction. Building on this insight, we develop an algorithm that estimates the pointing direction using UWB readings from a single anchor. The second challenge is mapping the estimated pointing direction to specific IoT devices, which requires knowledge of their locations relative to the anchor. A straightforward approach would be to manually measure the position of each IoT device, but this is impractical, especially in a 3-D space where precise measurements can be cumbersome. To address this, we propose a user-friendly localization method: when a new IoT device appears, our design enables the user to “tell” the system where this device is located by simply pointing at it twice at two distinct locations. By analyzing the two pointing directions, we can estimate the IoT device’s location at their intersection. This approach significantly reduces setup effort while ensuring adaptability to real-world deployments.

To validate our approach, we implement PnPSelect on several commercial devices and conduct comprehensive experiments. We benchmark the accuracy of pointing direction estimation and IoT device selection in controlled lab settings. We then deploy our system in real-world environments and conduct user studies to evaluate its practical effectiveness. The main contributions of this work are summarized below:

- We present PnPSelect, an IoT device selection solution that eliminates the need for dedicated hardware on each IoT device, enabling true plug-and-play functionality.

- We propose a pointing direction estimation algorithm that allows users to select IoT devices using a single UWB anchor. We develop a user-friendly IoT device localization approach, requiring only two pointing gestures to estimate device locations accurately.
- We prototype our design and showcase the effectiveness of the proposed system with both benchmark and real-world experiments. Comprehensive experiments demonstrate its superior performance in terms of accuracy and deployment flexibility.

2 Background and Related Work

In this section, we first present the background knowledge of UWB technology and its use on commodity devices. Then, we review existing IoT device selection solutions and highlight the difference between our proposed design and related work.

2.1 Background of UWB

UWB is a wireless technology characterized by its large frequency bandwidth, typically exceeding 500 MHz or 20% of its center carrier frequency [34]. With such a large bandwidth, the UWB device can distinguish most multipath signals in the environment, enabling highly accurate Time-of-Arrival (ToA) measurements between UWB-equipped devices. Thus, compared to narrowband signals (e.g., Wi-Fi and Bluetooth), UWB is more suitable for precise device localization even in a multipath-rich environment [29]. Currently, three methodologies can be used for UWB-based localization [44], including ToF [1, 29, 32], Time-Difference-of-Arrival (TDoA) [25, 26, 43], and AoA [13, 23, 50]. ToF-based localization estimates the distance between the target device and multiple anchors based on ToA measurements. By triangulating these distances, the device’s position can be determined. TDoA-based approaches utilize the ToA differences between multiple anchors to compute the device’s position. It should be noted that both ToF and TDoA-based solutions require multiple anchors for localization, i.e., more than two anchors. AoA-based methods, in contrast, use an antenna array to measure the Phase-Difference-of-Arrival (PDoA), enabling angle estimation. By combining distance and angle measurements, AoA-based localization can accurately determine a device’s position with just a single anchor.

In recent years, advancements in UWB technology, coupled with reductions in hardware cost and size, have led to its widespread integration into consumer electronic devices. Major manufacturers, including Apple [8], Samsung [6], Xiaomi [3], and Google [5], have incorporated UWB modules into their smartphones to enable precise device positioning. Additionally, various smart devices, such as Apple Watch, Apple HomePod, Apple TV, Apple AirPods Pro, and Mi TV, are now equipped with UWB capabilities. Thanks to its high-precision distance and angle estimation capability [22], UWB has been widely adopted for applications including tracking [28, 44, 53], item positioning [4, 41], and digital keys [52]. A well-known smart home application involves using a UWB-equipped iPhone to locate an AirTag, where the phone precisely measures both the distance and angle of the tag for object tracking [4]. Beyond traditional positioning tasks, recent research has explored UWB’s potential in contactless sensing [17, 18, 27, 45, 46, 51]. Furthermore, UWB hardware manufacturers have released development kits capable of establishing UWB connections with both Apple and Android smartphones [7, 9], offering new possibilities for customized UWB-based applications. In this paper, we leverage UWB-equipped smartphones and smartwatches as user devices to implement our IoT device selection system, enabling intuitive and seamless interaction without requiring additional hardware on IoT devices.

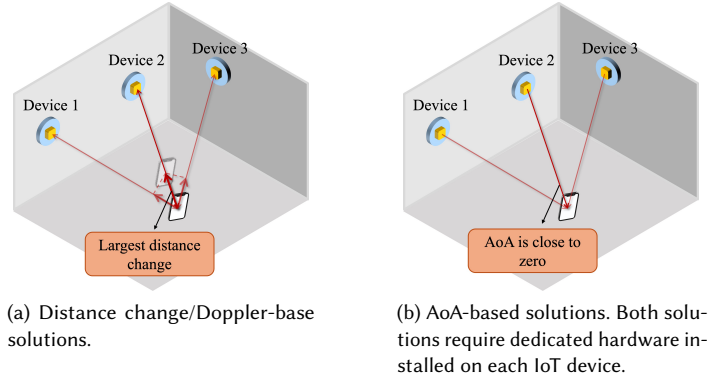


Fig. 2. Illustration of existing wireless signal-based IoT device selection techniques.

2.2 IoT Device Selection Techniques

With the rapid expansion of IoT ecosystems, researchers have explored various solutions to simplify IoT device selection and control. Some approaches [38, 42, 48, 49] rely on gesture-based interactions, requiring users to perform specific movements to select and control devices. However, as the number of IoT devices in an environment increases, memorizing a large set of gestures becomes impractical. To enhance usability, alternative methods focus on more intuitive interactions, allowing users to select a device simply by pointing at or looking at it. Various devices have been leveraged for this purpose, including smartwatches [12], earphones [40], smart glasses [47], and smartphones [30, 33]. Among these, camera-based approaches enable selection by capturing an image of the target device [16, 19] or tapping on a previewed object on a screen [15, 39]. Other methods utilize eye gaze tracking [30, 31], while recent work [33] combines device recognition with eye-gaze estimation to determine which device the user is viewing. However, camera-based solutions suffer from poor performance in low-light conditions and difficulty distinguishing visually similar devices, limiting their practicality [35]. To overcome these challenges, wireless signal-based approaches have been proposed, leveraging signal properties such as ToF and AoA measurements to enable device selection. These methods utilize signals like Bluetooth [47], UWB [12], and acoustic waves [14, 37, 40]. In general, wireless signal-based selection techniques fall into two categories, including distance change/Doppler-based solutions [12, 14, 37] and AoA-based solutions [40, 47]. As shown in Figure 2a and 2b, both types of systems require each IoT device to be equipped with the same type of wireless module to establish a connection with the user's device for distance or angle measurements.

Distance change/Doppler-based Solutions. These methods measure how the distance between the user device and each IoT device changes during the pointing gesture. As illustrated in Figure 2a, the key insight is that the distance to the target device exhibits the most significant change, allowing it to be identified. For example, SeleCon [12] measures distance variations between a smartwatch and IoT devices using UWB signals. Alternatively, Doppler-based approaches infer motion by measuring frequency shifts in signals caused by movement. Since the Doppler shift is a direct consequence of distance change, both methods provide similar insights. Doplink[14] and Spartacus[37] leverage acoustic signals to measure Doppler shifts, enabling smartphone-based IoT device selection.

AoA-based Solutions. AoA-based techniques extract the angle of incoming signals transmitted by IoT devices to determine which device the user is pointing at. As shown in Figure 2b, the AoA of the target device is closest to zero in

the view of the user device, making it possible to identify the intended selection. BLEselect [47] designs an antenna array on smart glasses to estimate the AoA of Bluetooth signals emitted by IoT devices in the environment, determining which IoT device the user is pointing at or looking at. FaceOri [40] employs microphones on the earphone to measure the AoA of acoustic signals emitted from nearby speakers on laptops, enabling detection of which laptop the user is facing.

Limitations of Existing Wireless Signal-based Methods. Regardless of the underlying approach, current wireless signal-based solutions require every IoT device to be equipped with a dedicated wireless module, making them impractical for real-world deployment due to cost and scalability concerns. In contrast, our method removes the need for additional hardware on each IoT device by proposing a novel device selection scheme using UWB signals. Our approach requires only a single UWB anchor in the environment, enabling room-level IoT device selection without modifying existing smart home appliances. By removing the requirement of installing additional hardware on each IoT device, our system offers a scalable and easily deployable solution for real-world IoT interactions.

3 Principle of Single Anchor-based Device Selection

In this section, we propose the detailed principle of single UWB anchor-based IoT device selection. Specifically, we do not expect any dedicated UWB hardware to be installed on IoT devices as existing solutions (Figure 2). Instead, as shown in Figure 3, only one UWB-equipped device is placed in the environment, serving as a UWB anchor.

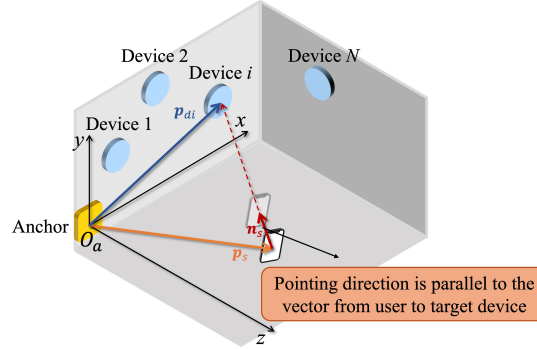


Fig. 3. Illustration of PnPSelect. Only one anchor is required in the environment.

3.1 Fundamental Principle of PnPSelect

Figure 3 illustrates the core concept behind our single anchor-based IoT device selection design. Imagine a user interacting with the system: they point at the desired device by moving their smartphone or smartwatch in a natural gesture. The key insight is that the direction of the pointing gesture should closely align with the direction from the user device to the target IoT device. In other words, the pointing direction and the vector connecting the user device to the target device should be parallel. Based on this principle, PnPSelect follows two essential steps for device selection.

The first step is estimating the pointing direction of the user device. Since the system does not rely on dedicated transceivers on IoT devices, we develop a UWB-based pointing direction estimation algorithm using the readings reported by a single anchor. As shown in Figure 3, we define an anchor coordinate system (C_a) bound to the anchor

fixed in the environment. The vector of the pointing direction is denoted as \mathbf{n}_s . We will introduce pointing direction estimation in Section 3.2.

The second step is identifying the target IoT device by computing the direction vectors from the user device to all IoT devices. Then, the device whose direction best matches the estimated pointing direction in the first step is selected as the desired target. As shown in Figure 3, the location of the user device (e.g., a smartphone) is denoted as \mathbf{p}_s . Then, the vector from the location of the user device to the i -th IoT device is $\mathbf{p}_{di} - \mathbf{p}_s$, where \mathbf{p}_{di} denotes the location of the i -th IoT device in C_a . Thus, a crucial requirement for the second step is knowledge of each IoT device's location (\mathbf{p}_{di}), which presents a non-trivial challenge in real-world deployments. We address this issue by introducing a lightweight and user-friendly device localization method, detailed in Section 3.3.

3.2 Pointing Direction Estimation

Traditional methods for estimating a user's pointing direction often rely on Inertial Measurement Unit (IMU) sensors, including accelerometers, gyroscopes, and magnetometers. One common approach is to use accelerometers and gyroscopes to infer the device's motion direction. However, this method only provides the direction of device motion relative to the device's own coordinate system, rather than a global reference coordinate system bound to the real-world environment (e.g., C_a). As a result, pointing direction estimation based solely on accelerometers and gyroscopes is insufficient for IoT device selection, as it does not provide the absolute pointing direction in 3-D space. An alternative approach is to use magnetometers to estimate absolute orientation by referencing the Earth's magnetic field. However, magnetic fields from ferromagnetic objects in the indoor environment and ferromagnetic components inside the smartphone can interfere with the measurement of the magnetometer, resulting in inaccurate orientation estimation [20]. Even when deep learning-based approaches are employed to compensate for these distortions, the orientation estimation error remains as high as 8.02° [36]. In dense IoT environments where precise pointing direction estimation is required, such an error margin is unacceptable. For example, if two IoT devices are placed 30 cm apart, and a user points at one of them from 3 m away, the angular separation between the two devices is only 5.7° . A higher orientation estimation error would make it impossible to reliably distinguish which device the user is pointing at, leading to ambiguous or incorrect selections. Moreover, a device's physical orientation does not always align with the direction of a pointing gesture performed by a user. When holding a smartphone or smartwatch, users inevitably tilt, rotate, or shift their devices slightly in 3-D space, meaning that the device's orientation does not necessarily align with the intended pointing direction. Given these issues, we do not rely on IMU sensors for pointing direction estimation. Instead, we develop a

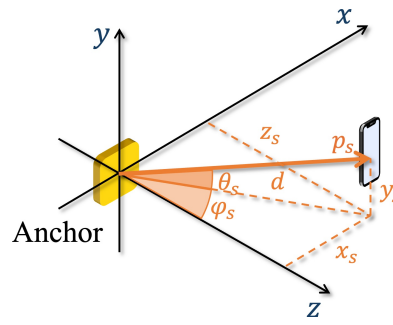


Fig. 4. Location estimation with a single anchor.

UWB-based approach that leverages UWB readings reported by a single anchor to infer the pointing direction of the user device.

The key insight behind our solution is that when a user performs a pointing gesture, the trajectory of the device's movement can be captured through UWB-based localization. By analyzing this trajectory, we can accurately infer the pointing direction of the user device. First, we describe how the trajectory is acquired using UWB localization. As introduced in Section 2.1, three schemes, i.e., ToF, TDoA, and AoA, can be used for localization. Among these, AoA-based methods are particularly suitable for our design since they require only one anchor. Accordingly, we employ AoA-based location estimation in our system. The distance (d) between the user device and the anchor is estimated using two-way-ranging (TWR) techniques [1, 32]. Simultaneously, the azimuth angle (φ_s) and elevation angle (θ_s) of the user device relative to the anchor are measured using multiple antennas on the anchor [23, 50]. As illustrated in Figure 4, these measurements allow us to compute the location of the user device in the anchor coordinate system C_a as follows:

$$\begin{aligned} \mathbf{p}_s &= (x_s, y_s, z_s)^T \\ &= (d \cos \theta_s \sin \varphi_s, d \sin \theta_s, d \cos \theta_s \cos \varphi_s)^T. \end{aligned} \quad (1)$$

By continuously estimating the user device's location, we obtain a series of position samples over time, forming a trajectory in 3-D space. Figure 5 illustrates an example trajectory recorded when the user points at an IoT device. The dominant movement direction along this trajectory corresponds to the user's pointing direction. A straightforward way to estimate the motion direction is by computing displacement vectors between consecutive location samples and averaging them. However, this method is susceptible to random errors arising from two main sources. The first arises from involuntary hand movements, which cause slight deviations from the intended pointing direction. The second is the UWB localization error, which introduces small inaccuracies in location estimation. To address these issues, we first apply a Kalman Filter [24] to smooth the trajectory, mitigating fluctuations and improving robustness. We then formulate the pointing direction estimation as an optimization problem:

$$\arg \max_{\mathbf{n}_s} \sum_{m=1}^M [\mathbf{n}_s \cdot \mathbf{p}_s(m)]^2, \quad (2)$$

where M is the number of location samples in the trajectory, and $\mathbf{p}_s(m)$ represents the location of the m -th sample. This optimization finds the direction vector \mathbf{n}_s that maximizes the variance when the trajectory is projected onto it,

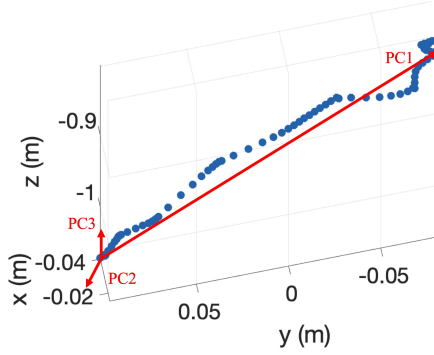


Fig. 5. The trajectory of a user device during pointing. PCA can be used to estimate the direction of pointing.

ensuring that the estimated direction aligns with the dominant movement trend. To solve this problem, we employ Principal Component Analysis (PCA), which uses an orthogonal transformation to identify the direction along which the data exhibits the largest variance. The first principal component (PC1) is extracted as the pointing direction, while PC2 and PC3 which correspond to noise and other deviations are discarded. As illustrated in Figure 5, this approach ensures that only the primary motion trend is retained, leading to accurate and stable pointing direction estimation.

3.3 IoT Device Selection

So far, we have obtained the pointing direction (\mathbf{n}_s) of the user device. The next step is to determine which IoT device the user is pointing at. However, before identifying the specific device, we must first obtain the locations of all IoT devices in the environment. Assume there are N IoT devices, and the location of the i -th IoT device in the anchor coordinate system C_a is denoted as $\mathbf{p}_{di} = (x_{di}, y_{di}, z_{di})^T$. For device selection to be feasible, these locations must be known in advance.

3.3.1 IoT Device Location Estimation. A straightforward approach is to manually measure and record each IoT device's position. However, this is impractical and labor-intensive, particularly since it requires measuring the relative 3-D positions of all IoT devices with respect to the anchor coordinate system C_a . An alternative approach is to simply place the user device on the new IoT device and record its position using UWB localization. In this case, the measured location of the user device would correspond to the IoT device's position. However, this method has several limitations due to the varying spatial relationships between IoT devices and the anchor. In many scenarios, an IoT device may be located outside the FoV of the anchor, making direct localization inaccurate or impossible. For instance, if the anchor is mounted on a wall, IoT devices installed on the same wall may fall outside the anchor's typical 120° FoV. Similarly, if the anchor is embedded in a smart TV, IoT devices positioned behind the TV would be out of the FoV. Moreover, in some cases, direct line-of-sight (LoS) between the anchor and the IoT device may be obstructed by objects in the environment, leading to significant localization errors.

To overcome these challenges, we propose a novel and user-friendly solution that allows accurate estimation of an IoT device's position relative to the anchor, regardless of its placement. Our method is designed to be robust to different placement conditions, ensuring reliable localization in real-world environments. Intuitively, the key idea of our approach is to let the user point at the device to "tell" the system where it is. As shown in Figure 6a, the smartphone

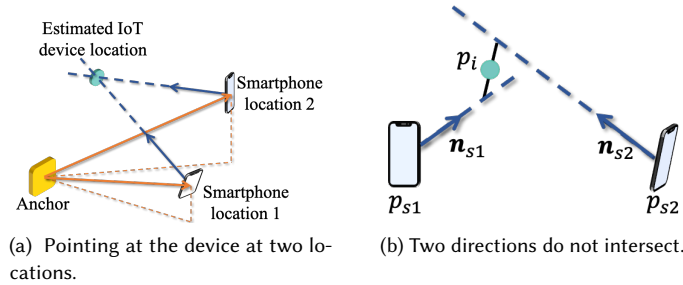


Fig. 6. Illustration of IoT device location estimation. The user can point at the device at two locations to "tell" the system where the device is. In the case where two pointing directions do not intersect, the point closest to two directions is estimated as the device location.

points at an IoT device whose location is unknown. Then, it can be determined that this device is on the line of the pointing direction. However, this is not sufficient, because any location on this line is a possible location for this device. To this end, we let the user point at the device again at another location to obtain another line containing the possible location. The intersection of the two lines is thus the location of the IoT device. Considering that the shape of an IoT device is not a point in reality, in 3-D space, the two straight lines may not have an intersection as shown in Figure 6b. We then obtain the shortest distance connecting the two lines and pick the middle point of the connecting line as the device location. Let $\mathbf{p}_{s1} = (x_{s1}, y_{s1}, z_{s1})^T$ and $\mathbf{p}_{s2} = (x_{s2}, y_{s2}, z_{s2})^T$ denote the location of the smartphone when it is pointed at the i -th device twice. $\mathbf{n}_{s1} = (e_{x1}, e_{y1}, e_{z1})^T$ and $\mathbf{n}_{s2} = (e_{x2}, e_{y2}, e_{z2})^T$ are the corresponding pointing direction vectors. Then, the equations of the line in which the two directions the smartphone is pointing at are:

$$\begin{aligned} \mathbf{p}_1 &= \mathbf{p}_{s1} + t_1 \cdot \mathbf{n}_{s1}, \\ \mathbf{p}_2 &= \mathbf{p}_{s2} + t_2 \cdot \mathbf{n}_{s2}, \end{aligned} \quad (3)$$

where t_1 and t_2 are variable parameters and different values can be substituted to obtain different locations (e.g., \mathbf{p}_1 and \mathbf{p}_2) on the lines. To calculate the location of the intersection of two lines or the point closest to the two lines, the following equation can be solved using the least squares method [21]:

$$\begin{bmatrix} t_1 \\ t_2 \end{bmatrix} = (M^T M)^{-1} M^T B, \quad (4)$$

$$\text{where } M = \begin{bmatrix} e_{x1} & -e_{x2} \\ e_{y1} & -e_{y2} \\ e_{z1} & -e_{z2} \end{bmatrix} \text{ and } B = \begin{bmatrix} x_{s2} - x_{s1} \\ y_{s2} - y_{s1} \\ z_{s2} - z_{s1} \end{bmatrix}.$$

Consequently, the estimated location of IoT device can be obtained by substituting t_1 and t_2 to Equation 3 as:

$$\mathbf{p}_{di} = \frac{1}{2}(\mathbf{p}_1 + \mathbf{p}_2) = \frac{1}{2}(\mathbf{p}_{s1} + t_1 \cdot \mathbf{n}_{s1} + \mathbf{p}_{s2} + t_2 \cdot \mathbf{n}_{s2}). \quad (5)$$

Therefore, whenever a new IoT device joins the system, we can estimate the location of that device using the above approach. Meanwhile, the location of each device can be updated when the IoT device location changes, improving the robustness of the proposed system in real-world settings.

3.3.2 Identifying Target IoT Device. At this stage, we have obtained the 3-D location of each IoT device relative to the anchor. It is important to note that IoT device location estimation is only required when a new device is introduced into the environment or when its placement changes. Once an IoT device's position has been estimated, it is recorded and reused for subsequent pointing-based selection, eliminating the need for repeated localization. The fundamental principle behind IoT device selection is that the direction vector of the user device's pointing gesture should align with the direction vector from the user device to the target IoT device. Based on this, we first compute the unit direction vectors from the user device to all IoT devices. The direction vector to the i -th IoT device is expressed as:

$$\begin{aligned} \mathbf{n}_i(m) &= (e_{ix}, e_{iy}, e_{iz})^T = \mathbf{p}_{di} - \mathbf{p}_s(m) \\ &= \frac{(x_{di} - x_s(m), y_{di} - y_s(m), z_{di} - z_s(m))^T}{\sqrt{(x_{di} - x_s(m))^2 + (y_{di} - y_s(m))^2 + (z_{di} - z_s(m))^2}}, \end{aligned} \quad (6)$$

where m represents the index of a location sample in the trajectory. As illustrated in Figure 7, when the user device is pointing at the i -th IoT device, the pointing direction vector (\mathbf{n}_s) is expected to be identical to the unit vector $\mathbf{n}_i(m)$. This condition can be expressed as $\mathbf{n}_s \cdot \mathbf{n}_i(m) = 1$. However, in practical scenarios, IoT devices are not point-like objects

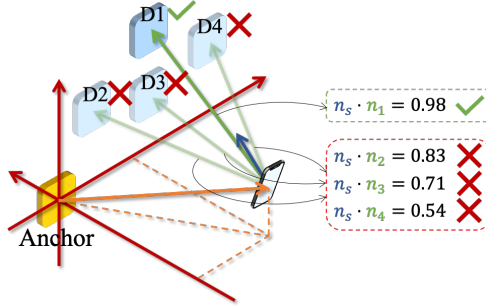


Fig. 7. Illustration of device selection based on pointing direction estimation.

but rather have physical dimensions, which means that the calculated directional similarity may not be exactly 1 but should be close to 1 as shown in Figure 7. To account for this, we systematically search through all IoT devices to identify the one most likely being pointed at by the user. Since multiple location samples are collected while the user performs the pointing gesture, we incorporate all trajectory samples to enhance robustness against random localization errors. The selection process is formulated as the following minimization problem:

$$\arg \min_i \sum_{m=1}^M |1 - \mathbf{n}_s \cdot \mathbf{n}_i(m)|/M. \quad (7)$$

By minimizing this expression, we identify the IoT device whose direction vector best matches the user's pointing direction, effectively achieving robust and accurate selection based on pointing gestures.

4 Implementation

To validate our design, we implement our system on both Apple and Android platforms. For evaluations involving Apple devices, we employ an iPhone 11 as a fixed anchor within our test environments. Users interact with the system using either an iPhone 12 Pro Max or an Apple Watch Series 6 to select IoT devices. To facilitate UWB-based measurements, we develop an iOS application utilizing Apple's Nearby Interaction framework [8], which enables peer-to-peer UWB communication between two iPhones or between an iPhone and an Apple Watch. This framework provides real-time distance and angle measurements, which form the basis of our system's pointing direction estimation. Our experiments reveal that the UWB data reporting rate for Apple devices is 55 Hz, ensuring a high-frequency stream of spatial data. The extracted distance and angle information from the Nearby Interaction framework is transmitted via a TCP connection to a server laptop (a MacBook Pro equipped with an Apple M3 Max CPU and 32GB RAM) for further processing and evaluation. In addition to Apple's ecosystem, Android also supports UWB-based measurements through its dedicated UWB API [10]. To evaluate our system on the Android platform, we utilize two Xiaomi Mix 4 smartphones, where one acts as the anchor and the other serves as the user device. During the pointing gesture, the anchor continuously measures the distance and angle of the user device. These measurements are stored in a local file on the anchor and later transmitted to the laptop for further data processing and analysis.

5 Evaluation

In this section, we first conduct benchmark experiments to understand the pointing direction estimation performance of our solution. The impact of several parameters is evaluated in the benchmark experiments. The results help us

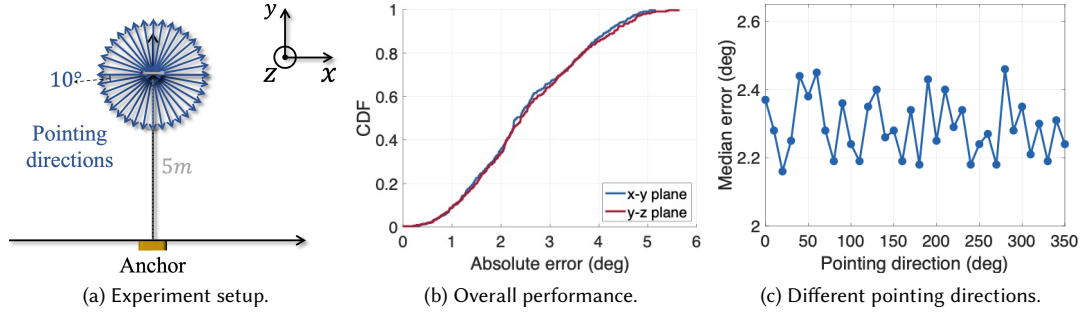


Fig. 8. Overall performance and impact of pointing direction.

understand the capability of single anchor-based pointing direction estimation and shed light on guiding the system development. Then, we evaluate our system in various real-world environments to demonstrate the performance of IoT device selection.

5.1 Accuracy of Pointing Direction Estimation

5.1.1 Experiment Setting. The core of our system design is the estimation of user device's pointing direction. Therefore, we first conduct benchmark experiment on pointing direction estimation and evaluate the impact of several parameters. We fix the anchor in the environment and then vary the location and pointing direction of the user device (i.e., a smartphone). The smartphone is mounted on a sliding track, the displacement and velocity of which can be precisely controlled. This setup allows us to use the sliding track to manage the smartphone's movements, thereby simulating the pointing gesture.

5.1.2 Impact of User Device Pointing Direction. We evaluate the estimation accuracy under different pointing directions. As illustrated in Figure 8a, the initial distance between the user device and the anchor is set at 5 m. We then use the sliding track to move the user device at a speed of 0.1 m/s over a distance of 20 cm to simulate the “pointing” gesture. We traverse a full 360° of pointing directions at a step of 10° and use our proposed algorithm to estimate the direction. It should be noted that the pointing direction vector is 3-D in space. Thus, besides the setting shown in Figure 8a, in which the pointing direction is in the x-y plane, we also repeat the experiment when it is in the y-z plane. Figure 8b shows the overall direction estimation errors using the data collected under all parameters. For the movement in x-y plane, the median error and the 90-percent error of our design are 2.33° and 4.20°, respectively. For the movement in y-z plane, the median error and the 90-percent error are 2.39° and 4.32°, respectively. Figure 8c shows the median estimation error for each direction in both settings. It is evident that the median error remains below 2.46° across all directions, with no significant variation between different directions. This experiment confirms that the estimation error is similar and less than 2.46° when pointing in different directions with the user device's position fixed. Meanwhile, the performance under two settings is similar, indicating that our solution can be used to measure 3-D pointing direction accurately.

5.1.3 Impact of User Device Location. In this experiment, we evaluate the impact of user device location on pointing direction estimation. Specifically, we decompose the location into two parameters, which are the distance and angle of the user device with respect to the anchor. As shown in Figure 9a, we vary the distance between the user device and the anchor from 1 m to 5 m at a step of 1 m. At each distance, we move the user device from -50° to 50° at a step of 10°. We

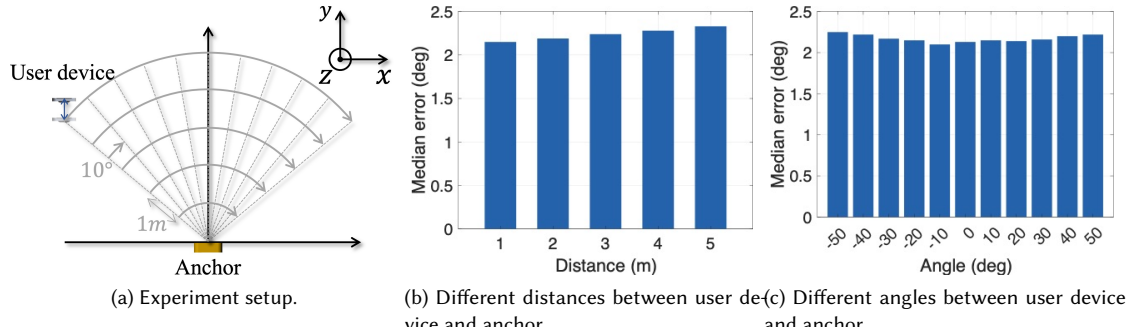


Fig. 9. Impact of user device location.

calculate the median error between the estimated value and ground truth. Figure 9b and 9c show the impact of distance and angle between the user device and anchor. Although we find that the pointing direction error slightly increases with the angle and distance of the user device with respect to the anchor, for all locations of the user smartphone, the median direction estimation error is lower than 2.33° . These results show that our design can achieve a high direction estimation accuracy in the typical home-size environments.

5.1.4 Impact of the Displacement of Pointing. In reality, different users may exhibit various pointing gesture patterns, leading to distinct displacements while performing the gesture. Moreover, even the same individual is likely to experience variations in displacement during usage. Therefore, in this experiment, we evaluate the impact of different pointing gesture displacements on direction estimation. We set six different displacements ranging from 5 cm to 30 cm at a step of 5 cm. As shown in Figure 10a, when the displacement is 5 cm, the error of direction estimation is 3.40° . When the displacement is 10 cm or more, the error significantly decreases and stabilizes at below 2.68° . This indicates that a longer displacement helps enhance the accuracy of direction estimation because it better mitigates the random offsets of the hand movement and measurement errors. Notably, as long as the displacement exceeds 10 cm, the system can ensure an error sufficiently small, under 2.68° . A movement of 10 cm is easily achievable. We also present the distribution of displacement sizes of multiple users actually utilizing the system in Section 5.3.3.

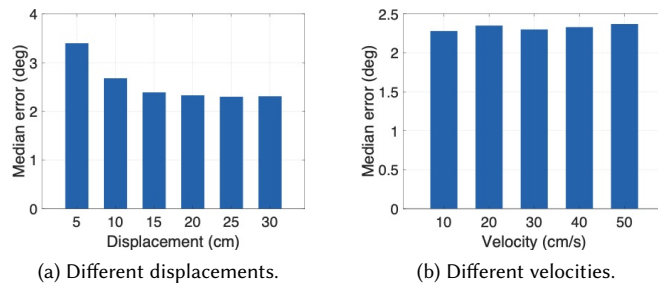


Fig. 10. Impact of the displacement and the velocity of pointing.

5.1.5 Impact of the Velocity of Pointing. Similar to the displacements evaluated in the previous section, the velocity of pointing gestures by users when using the system also varies significantly. Therefore, in this experiment, we evaluate the impact of different pointing gesture velocities on direction estimation. We evaluate five different velocities ranging from 10 cm/s to 50 cm/s, at a step of 10 cm/s. As illustrated in Figure 10b, for all velocities, the direction estimation error remains below 2.37°, and there is no significant difference in errors across different velocities. This indicates that varying gesture speeds have a minimal impact on direction estimation. The distribution of speeds of multiple users in real-world conditions is also presented in Section 5.3.3.

5.2 Evaluation on Spatial Resolution and Device Selection Accuracy

In real-world smart home environments, IoT devices may be densely placed. Therefore, a crucial factor in determining the effectiveness of the system is its spatial resolution. Suppose there are two closely positioned IoT devices. The key question is the minimum distance at which the system can accurately discern and select one device when the user points at it. We define this minimum distance as the spatial resolution. Intuitively, this spatial resolution is closely related to the accuracy of the pointing direction estimation. Based on the benchmark experiments in the previous sections, we know that the pointing direction estimation accuracy is approximately 2.36°, regardless of the positions of the anchor and user device or the pointing direction. This means that if the angle difference between two IoT devices relative to the user device is less than 2.36°, the system is likely unable to distinguish which device the user is actually pointing at. As shown in Figure 11a, with a fixed direction estimation accuracy, the spatial resolution enlarges as the distance between the user device and the IoT devices increases. Note that a larger spatial resolution indicates a worse device selection performance. Setting the direction estimation accuracy at 2.36°, we plot the theoretical spatial resolution at different distances in Figure 11b. It can be seen that, theoretically, two IoT devices spaced 20.6 cm apart at a distance of 5 m from the user device can be distinguished. In common smart home settings, this level of resolution is acceptable. In this section, we validate the spatial resolution through several experiments to confirm its alignment with theoretical predictions.

5.2.1 Impact of Distance Between User Device and IoT Device. In this section, we evaluate the spatial resolution of our system under various settings. As shown in Figure 12a, the distance between the user device and the anchor is fixed at 5 m. We vary the distance between the user device and the IoT device (i.e., d) from 1 m to 5 m at a step of 1 m. At each distance, two items, each with a size of 3cm × 3cm × 6cm, are used to represent two IoT devices. We gradually reduce the distance between the two items until the average selection accuracy is below 90%. This distance is then defined as

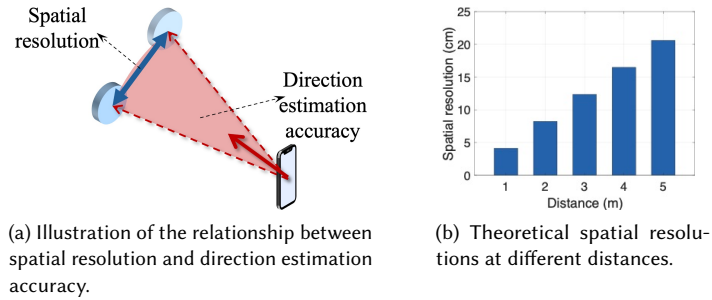


Fig. 11. Evaluation on spatial resolution.

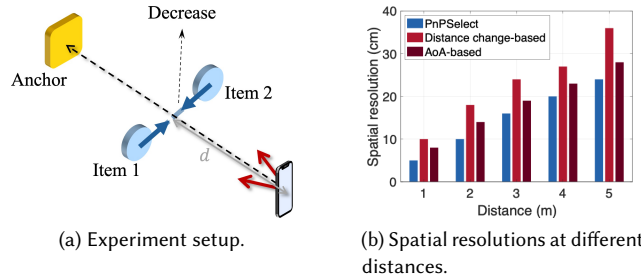


Fig. 12. Impact of distance between user device and IoT device on spatial resolution.

the spatial resolution at this distance. Simultaneously, we compare our system with two baseline methods: Selecon [12], a distance change-based solution and BLEselect [47], an AoA-based solution. Note that BLEselect [47] is implemented using Bluetooth signals. However, Bluetooth-based systems typically exhibit higher inaccuracies in AoA estimation compared to UWB-based systems, since Bluetooth works with a much smaller bandwidth than UWB. Thus, to ensure a fair comparison, we implement the AoA-based method using UWB instead of Bluetooth. In this way, the hardware and the UWB data used for our design, the distance change-based solution, and the AoA-based solution are identical. The only difference lies in the processing approach of the UWB data for device selection. Meanwhile, UWB anchors should be attached to both items when implementing the baseline approaches, while PnPSelect only requires one anchor in the environment.

Figure 12b illustrates the spatial resolutions of the three approaches at varying distances. At the five different distances, the spatial resolutions of our method are 5 cm, 10 cm, 16 cm, 20 cm, and 24 cm, respectively, aligning with the theoretical analysis presented in Figure 11b. The spatial resolutions for the distance change-based approach are 10 cm, 18 cm, 24 cm, 27 cm, and 36 cm, while those for the AoA-based method are 8 cm, 14 cm, 19 cm, 23 cm, and 28 cm. These results demonstrate that our solution offers superior spatial resolution and cost-effectiveness, requiring only one anchor, thus outperforming existing solutions.

5.2.2 Impact of the IoT Device Location. In practical deployments, IoT devices may be positioned throughout various locations in a room. To this end, our experiment evaluates the impact of IoT device location on spatial resolution and

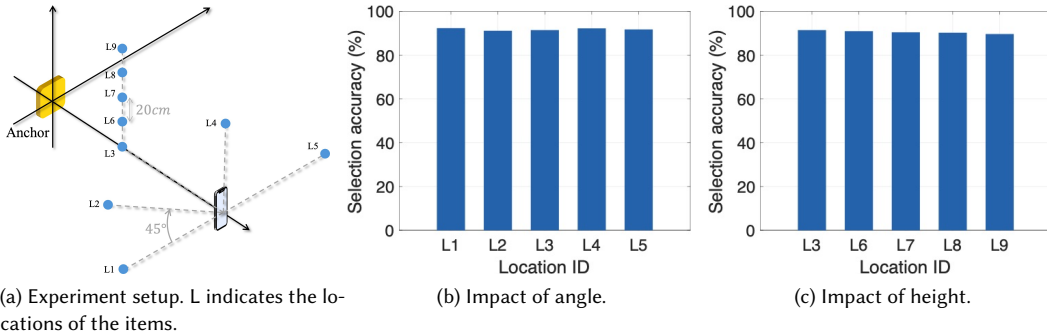


Fig. 13. Impact of IoT device location on device selection accuracy.

device selection accuracy. As shown in Figure 13a, we fix the distance between the anchor and the user device at 5 m. We evaluate nine different IoT device locations in total. Initially, we fix the distance between two items (simulating IoT devices) and the user device at 3 m, then change the angle of the two items relative to the user device at a step of 45°. Subsequently, using L3 as a reference, we move the two items upwards at a step of 20 cm. In all experiments, the distance between the two items is fixed at 16 cm, which is the spatial resolution at 3 m. We calculate the device selection accuracy at all different locations. As illustrated in Figure 13b, at five different angles, the device selection accuracy exceeds 91.2%. At five different heights, the device selection accuracy remains above 89.7% as shown in Figure 13c. These results demonstrate that our proposed method robustly functions under various IoT device placements.

5.3 Test in Real-world Environments

In this section, we evaluate our system in four real-world environments, including two bedrooms, a classroom, and a meeting room. In each environment, we select 10 common pieces of furniture or appliances as potential IoT devices. We first evaluate the accuracy of the proposed IoT device location estimation method, which is essential for real-world system development. Then, we evaluate the device selection accuracy within each setting. Additionally, we investigate the impact of several realistic parameters on accuracy, including different users, locations, pointing displacements and velocities, as well as various types of user devices.

5.3.1 Experiment setting. The four environments are shown in Figure 14 and are denoted as S1, S2, S3, and S4, respectively.

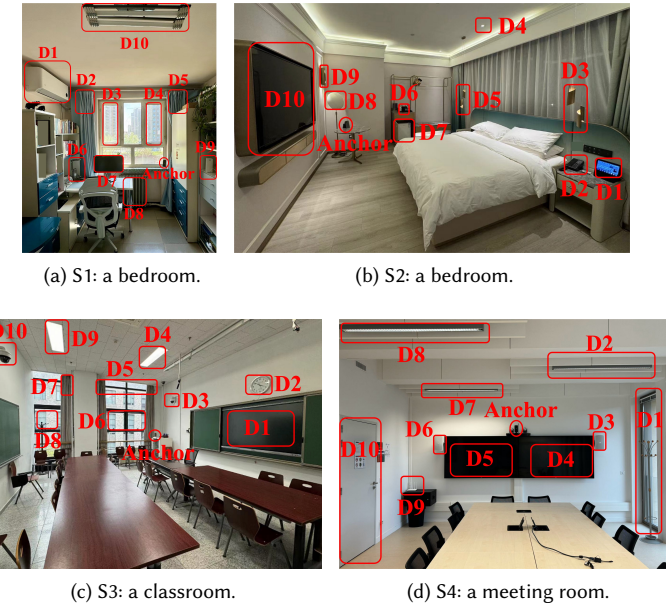


Fig. 14. Real-world scenarios.

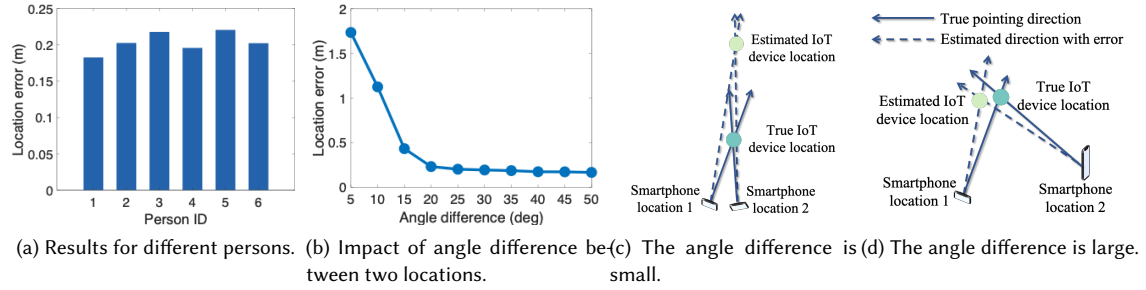


Fig. 15. Evaluation on IoT device location estimation.

S1: A small bedroom with a size of $2.8\text{ m} \times 3.8\text{ m}$. There are ten devices in the bedroom, including an air conditioner (D1), two curtains (D2 and D5), two windows (D3 and D4), two lights (D6 and D10), a monitor (D7), a heater (D8), and a router (D9).

S2: A large bedroom with a size of $4.1\text{ m} \times 5.0\text{ m}$. There are ten devices in this bedroom, including a smart speaker (D1), a telephone (D2), five lamps (D3, D4, D5, D8, and D9), a coffee machine (D6), a refrigerator (D7), and a TV (D10).

S3: A classroom with a size of $3\text{ m} \times 5.5\text{ m}$. There are ten devices in the classroom, including a monitor (D1), a clock (D2), two cameras (D3 and D10), two lights (D4 and D9), two curtains (D5 and D7), and two windows (D6 and D8).

S4: A meeting room with a size of $3.5\text{ m} \times 6\text{ m}$. There are ten devices in the meeting room, including a window (D1), three lights (D2, D7, and D8), two speakers (D3 and D6), two monitors (D4 and D5), a router (D9), and a door (D10).

In each environment, we recruit six participants to point at all devices at ten different locations. At each location, each participant points at each device five times. Thus, we collect a number of $6\text{ participants} \times 10\text{ locations} \times 5\text{ times} = 300$ data for each IoT device in an environment.

5.3.2 Evaluation on IoT Device Location Estimation. In this section, we conduct experiments to evaluate the effectiveness of the proposed IoT device location estimation scheme (Section 3.3.1). We conduct this experiment in S1 (Figure 14a). The groundtruth location of each IoT device with respect to the anchor is measured manually. We recruited six participants in this experiment. Each person is asked to point at each IoT device at ten locations in the room. We use data collected at two locations to estimate the location of the IoT device.

Figure 15a shows the IoT device location estimation errors for different persons. The mean error is lower than 0.23 m for all participants. Note that in a home scenario, the IoT devices have a certain size rather than a point, so the accuracy of our device location estimation scheme is acceptable. Then, we take a more detailed observation of the effect of user location during IoT device location estimation. Figure 15b shows the impact of the angle difference between two user locations when estimating the IoT device location. It can be seen that the IoT device location estimation error decreases with the increase of angle difference. When the angle difference is larger than 20° , the location estimation error tends to be stable and less than 0.23 m. Figure 15c and 15d illustrate the reason behind this observation. As shown in Figure 15c, when the angle difference between two smartphone locations are small, even slight pointing direction estimation error will induce large IoT device estimation error. In comparison, if the angle difference is significant (i.e., larger than 20°) as shown in Figure 15d, pointing direction error will not lead to large IoT device location estimation error. Note that when the distance between the user smartphone and the anchor is 4 m, as long as the distance between the two smartphone positions is greater than 1.4 m, the angle difference will be greater than 20° , thereby ensuring a low IoT device location

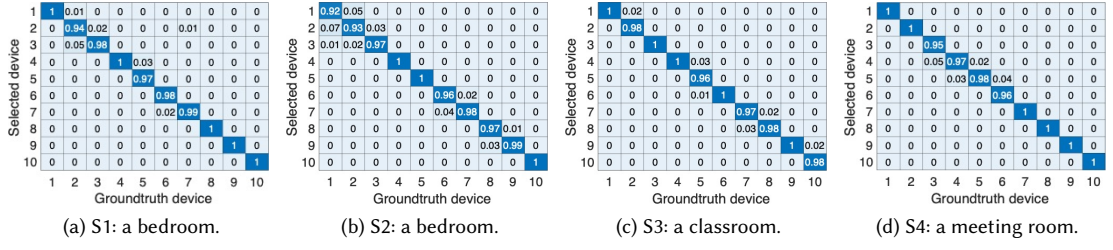


Fig. 16. Confusion matrices of IoT device selection in different environments.

estimation error. Therefore, the user only needs to change a small location (e.g., move two steps) to achieve accurate device location estimation. We discuss potential solutions to enhance user experience while ensuring high IoT device location estimation accuracy in Section 6.2.

5.3.3 Overall Performance of IoT Device Selection. We then conduct experiments to evaluate the accuracy of the proposed IoT device selection method. Note that in all environments, the location of each IoT device is estimated using our proposed scheme, rather than manual measurement. Figure 16 shows the confusion matrices of device selection in each environment. The average accuracy of device selection in four scenarios is 98.6%, 97.2%, 98.7%, and 98.6%, respectively. We further analyze the cases of incorrect selection. The reason for wrong selection is mainly due to the close proximity of IoT devices. Take D1 and D2 in S2 as an example. As shown in Figure 14b, when pointing at D1 near the D5, D2 is also close to the direction the smartphone is pointing at. We discuss potential solutions for this issue to enhance user experience in Section 6.2.

5.3.4 Impact of Anchor and User Location. We further evaluate the impact of anchor location in S4 (the meeting room). As shown in Figure 17a, we place the anchor at four different locations and repeat the above experiment. The result is shown in Figure 17b. When the anchor is placed at L1 and L4, the accuracy of device selection decreases compared to L2 and L3. This is because L1 and L4 are at the edge of the devices in the room. Therefore, when pointing at IoT devices, the user device is often at a larger distance, inducing a slight increment of pointing direction estimation error slightly (Section 5.1.3). However, regardless of the anchor's location, the selection accuracy consistently exceeds 96.1%. Figure 17c illustrates the device selection accuracy when the user is at ten different locations. Although we observe a

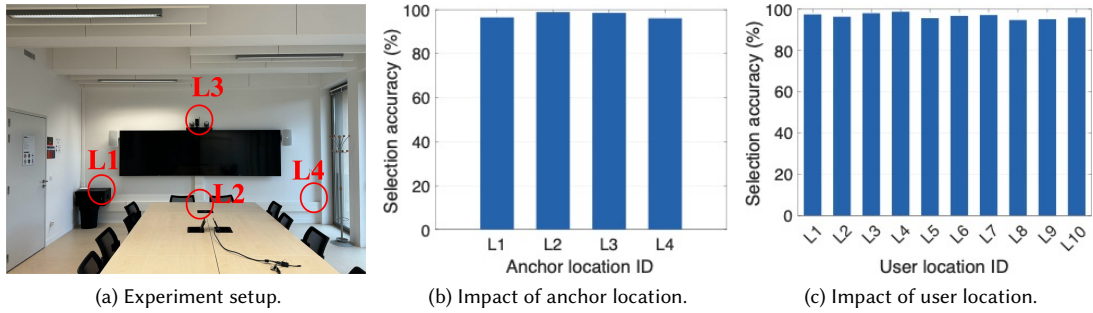


Fig. 17. Impact of anchor and user location.

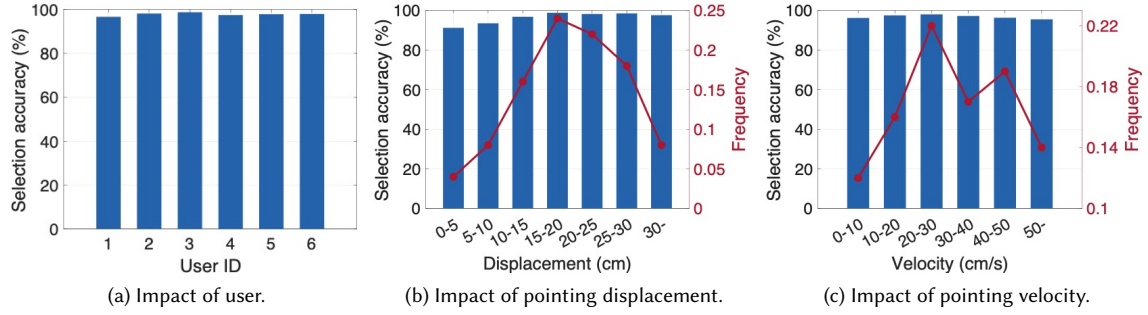


Fig. 18. Impact of user pointing patterns.

slight decrease in accuracy when the user is farther from the anchor, the average accuracy remains above 94.8%. These experiments demonstrate that our method maintains stable device selection performance across various anchor and user positions.

5.3.5 Impact of Pointing Patterns. In practice, different users may exhibit various pointing patterns, including differences in displacement and velocity. Additionally, even the same individual's pointing behavior may vary at different times. Therefore, in this experiment, we evaluate the impact of different users, pointing displacements, and pointing velocities. In S1, we test the device selection accuracy of six participants (four males and two females, ranging in height from 160 cm to 180 cm, and aged between 25 to 55 years). Figure 18a shows the average device selection accuracy for the six users exceeds 95.4% without significant differences. Subsequently, we further analyze the data from all users to calculate the accuracy of selection across different pointing displacements and velocities. Displacements are divided into seven intervals, each 5 cm wide. Figure 18b shows the frequency of displacements occurring within each interval and the device selection accuracy for each. The majority of user displacements are concentrated between 10 cm and 30 cm, where the device selection accuracy remains above 95.4%. We can observe that as displacements decrease below 10 cm, the accuracy of device selection declines (consistent with the findings in Section 5.1.4). Fortunately, the likelihood of displacements in this range is low. For velocities, we divide them into six intervals, each 10 cm/s wide. As shown in Figure 18c, there are no significant differences in device selection accuracy across different velocities.

5.3.6 Impact of Types of User Device. In this experiment, we evaluate the impact of different types of user devices on the accuracy of IoT device selection. In S1, we test three types of user devices, including an iPhone 12 Pro Max, an

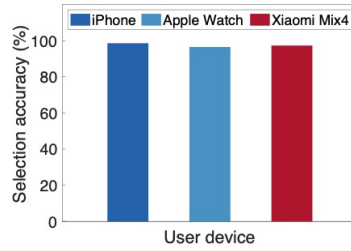


Fig. 19. Impact of types of user device.

Apple Watch S6, and a Xiaomi Mix 4. As shown in Figure 19, the selection accuracy for all three user devices was above 96.5%. This indicates that our method can operate stably across various user devices equipped with UWB.

6 Discussion and Limitation

6.1 System Generalization

6.1.1 Generalization Across User Devices. In this paper, we implement our system using the iPhone, Apple Watch, and Xiaomi Mix 4, due to the availability of detailed UWB reading extraction APIs provided by these devices. The latest UWB-equipped Google Pixel and Samsung smartphones also support the extraction of UWB data using Android APIs [10]. Additionally, we have observed that some of the newer models of Huawei watches and Apple earphones are equipped with UWB. Looking ahead, we expect that in the future, an increasing number of commercial devices will be incorporate UWB technology, including smart glasses, head displays, and smart rings, enabling the application of our design on a wide range of user devices.

6.1.2 Implementation of UWB Anchor. In this paper, we utilize a smartphone as the fixed UWB anchor in the environment. For real-world deployment, we envision two alternatives for the anchor. Firstly, the anchor can be realized by utilizing UWB-equipped smart devices. For example, smart speakers and TVs produced by Apple and Xiaomi have integrated UWB module. Currently, these manufacturers have not released the UWB data collection API for these smart devices. Alternatively, the UWB anchor can be implemented by leveraging third-party UWB chips and development boards [2, 7, 11]. These third-party UWB products can establish UWB connections with commercial smartphones and support data extraction, enabling our system design.

6.2 Enhancing User Experience

During our experiments, we identified two limitations in our proposed method that could affect user experience in real-world applications.

One limitation arises when estimating the location of a newly introduced IoT device. As introduced in Section 5.3.2, the user is required to point at the device from two distinct positions to establish sufficient angular separation between the two pointing directions. Specifically, the angle difference between the two pointing directions should be greater than 20°. If the angular separation is too small, the system may struggle to accurately estimate the IoT device’s position. To improve user experience, we propose incorporating user guidance mechanisms that assist in ensuring an adequate separation between the two pointing positions. First, we can leverage the UWB anchor to track the user’s location change between the two pointing gestures. If the detected displacement is less than 1.4 m, the system can prompt the user to move farther before performing the second pointing action. Second, we believe that an alternative approach could involve introducing small artificial perturbations in the IoT device location estimation (Equation 5). By analyzing the sensitivity of the IoT device’s estimated location to these perturbations, the system could determine whether the two pointing locations are too close. If minor errors in the input result in significant deviations in the estimated IoT device position (Figure 15c), the system could infer that the two locations lack sufficient separation and notify the user to reposition themselves accordingly. We believe that incorporating these mechanisms can ensure the accuracy of IoT device location estimation while maintaining a positive user experience.

Another limitation occurs when multiple IoT devices are located close to each other, making it difficult for the system to unambiguously determine which device the user intends to select. This issue is particularly problematic when two IoT devices are positioned extremely close to each other, i.e., below the system’s spatial resolution, or when multiple

devices lie along the user's pointing direction. For example, as illustrated in Figure 14b, when the user points at D1 near D5, D2 is also close to the pointing direction. In such cases, relying solely on Equation 7 to select a single device may lead to incorrect selections, negatively impacting user experience. To address this, we propose an interactive selection mechanism that displays multiple candidate devices instead of automatically selecting one. When the system detects that more than one IoT device is aligned with the pointing direction, it does not immediately determine a single target device but instead presents all possible candidates on the user's smartphone screen. This allows the user to manually confirm their selection, preventing accidental activations. In the example mentioned above, instead of automatically selecting a single device (D1 or D2), the application can display both D1 and D2, allowing the user to make a final selection. Compared to the traditional approach of displaying all IoT devices in the room (i.e., ten devices), presenting only the most probable two candidates significantly reduces the complexity of the selection process. Additionally, this design helps prevent incorrect selections, thereby enhancing the overall user experience and minimizing frustration caused by unintended device activations.

7 Conclusion

In this paper, we present a novel design for IoT device selection using UWB-equipped commercial devices, eliminating the need of installing dedicated hardware on each IoT device. The key innovation of our design lies in utilizing a single anchor to accurately estimate the user device's pointing direction. We also propose a novel design to address a critical issue, i.e., the pre-collection of IoT devices in the environment, in real-world deployment. To validate our system, we conduct comprehensive evaluations in both controlled lab settings and real-world environments. The results demonstrate the promising potential of the proposed system for real-world deployment. We believe that our technology can benefit a large range of HCI applications.

References

- [1] 2011. IEEE Standard for Local and metropolitan area networks—Part 15.4: Low-Rate Wireless Personal Area Networks (LR-WPANs). *IEEE Std 802.15.4-2011 (Revision of IEEE Std 802.15.4-2006)* (2011), 1–314. doi:10.1109/IEEEESTD.2011.6012487
- [2] 2020. *Ubitraq*. <https://www.qorvo.com/innovation/ultra-wideband/partners/ubitraq>
- [3] 2020. *Xiaomi Introduces Groundbreaking UWB Technology*. <https://blog.mi.com/en/2020/10/13/xiaomi-introduces-groundbreaking-uwb-technology/>
- [4] 2021. *Find your keys, wallet, and more with AirTag*. <https://support.apple.com/en-us/HT210967>
- [5] 2021. *Google reiterates that Pixel 6 will have UWB as it works to expand support in Android 13*. <https://9to5google.com/2021/08/25/google-pixel-6-uwb-mention/>
- [6] 2021. *What is Ultra-Wideband (UWB) technology on Samsung Phones? How is it helpful?* <https://www.smartprix.com/bytes/phones-with-uwb-ultrawideband-connectivity/>
- [7] 2023. *Murata Type2bp*. <https://www.murata.com/en-us/products/connectivitymodule/ultra-wide-band/nxp/type2bp>
- [8] 2023. *Nearby Interaction*. <https://developer.apple.com/documentation/nearbyinteraction>
- [9] 2023. *Qorvo QM33120W*. <https://www.qorvo.com/products/p/QM33120W>
- [10] 2023. *Ultra-wideband (UWB) communication*. <https://developer.android.com/guide/topics/connectivity/uwb>
- [11] 2024. *Murata Type2bp*. <https://www.murata.com/en-global/products/connectivitymodule/ultra-wide-band/nxp/type2hq>
- [12] Amr Alanwar, Moustafa Alzantot, Bo-Jhang Ho, Paul Martin, and Mani Srivastava. 2017. Selecon: Scalable iot device selection and control using hand gestures. In *Proceedings of the Second International Conference on Internet-of-Things Design and Implementation*. 47–58.
- [13] Aditya Arun, Shunsuke Saruwatari, Sureel Shah, and Dinesh Bharadia. 2023. XRLoc: Accurate UWB localization to realize XR deployments. In *Proceedings of the 21st ACM Conference on Embedded Networked Sensor Systems*. 459–473.
- [14] Md Tanvir Islam Aumi, Sidhant Gupta, Mayank Goel, Eric Larson, and Shwetak Patel. 2013. Doplink: Using the doppler effect for multi-device interaction. In *Proceedings of the 2013 ACM international joint conference on Pervasive and ubiquitous computing*. 583–586.
- [15] Sebastian Boring, Dominikus Baur, Andreas Butz, Sean Gustafson, and Patrick Baudisch. 2010. Touch projector: mobile interaction through video. In *Proceedings of the SIGCHI Conference on Human Factors in Computing Systems*. 2287–2296.
- [16] Kaifei Chen, Jonathan Fürst, John Kolb, Hyung-Sin Kim, Xin Jin, David E Culler, and Randy H Katz. 2018. Snaplink: Fast and accurate vision-based appliance control in large commercial buildings. *Proceedings of the ACM on Interactive, Mobile, Wearable and Ubiquitous Technologies* 1, 4 (2018),

1–27.

[17] Zhe Chen, Tianyue Zheng, Chao Cai, and Jun Luo. 2021. MoVi-Fi: motion-robust vital signs waveform recovery via deep interpreted RF sensing. In *Proceedings of the 27th Annual International Conference on Mobile Computing and Networking*. 392–405.

[18] Zhe Chen, Tianyue Zheng, and Jun Luo. 2021. Octopus: a practical and versatile wideband MIMO sensing platform. In *Proceedings of the 27th Annual International Conference on Mobile Computing and Networking*. 601–614.

[19] Adrian A de Freitas, Michael Nebeling, Xiang'Anthony' Chen, Junrui Yang, Akshaye Shreenithi Kirupa Karthikeyan Ranithangam, and Anind K Dey. 2016. Snap-to-it: A user-inspired platform for opportunistic device interactions. In *Proceedings of the 2016 CHI Conference on Human Factors in Computing Systems*. 5909–5920.

[20] Zhihui Gao, Ang Li, Dong Li, Jialin Liu, Jie Xiong, Yu Wang, Bing Li, and Yiran Chen. 2022. MOM: Microphone based 3D Orientation Measurement. In *2022 21st ACM/IEEE International Conference on Information Processing in Sensor Networks (IPSN)*. IEEE, 132–144.

[21] Lejia Han and John C Bancroft. 2010. Nearest approaches to multiple lines in n-dimensional space. *Crewes Res. Rep* 22 (2010), 1–17.

[22] Alexander Heinrich, Sören Krollmann, Florentin Putz, and Matthias Hollick. 2023. Smartphones with UWB: Evaluating the Accuracy and Reliability of UWB Ranging. *arXiv preprint arXiv:2303.11220* (2023).

[23] Milad Heydariaan, Hossein Dabirian, and Omprakash Gnawali. 2020. Anguloc: Concurrent angle of arrival estimation for indoor localization with uwb radios. In *2020 16th International Conference on Distributed Computing in Sensor Systems (DCOSS)*. IEEE, 112–119.

[24] Rudolph Emil Kalman. 1960. A new approach to linear filtering and prediction problems. (1960).

[25] Benjamin Kempke, Pat Pannuto, and Prabal Dutta. 2016. Harmonium: Asymmetric, bandstitched UWB for fast, accurate, and robust indoor localization. In *2016 15th ACM/IEEE International Conference on Information Processing in Sensor Networks (IPSN)*. IEEE, 1–12.

[26] Anton Ledergerber, Michael Hamer, and Raffaello D'Andrea. 2015. A robot self-localization system using one-way ultra-wideband communication. In *2015 IEEE/RSJ International Conference on Intelligent Robots and Systems (IROS)*. IEEE, 3131–3137.

[27] Siheng Li, Zhi Wang, Fusang Zhang, and Beihong Jin. 2021. Fine-grained respiration monitoring during overnight sleep using IR-UWB radar. In *International Conference on Mobile and Ubiquitous Systems: Computing, Networking, and Services*. Springer, 84–101.

[28] Junqi Ma, Zhaoxin Chang, Fusang Zhang, Jie Xiong, Jiazhi Ni, Beihong Jin, and Daqing Zhang. 2022. Involving ultra-wideband in consumer-level devices into the ecosystem of wireless sensing. In *Proceedings of the 28th Annual International Conference on Mobile Computing And Networking*. 758–760.

[29] Junqi Ma, Fusang Zhang, Beihong Jin, Chang Su, Siheng Li, Zhi Wang, and Jiazhi Ni. 2024. Push the Limit of Highly Accurate Ranging on Commercial UWB Devices. *Proceedings of the ACM on Interactive, Mobile, Wearable and Ubiquitous Technologies* 8, 2 (2024), 1–27.

[30] Sven Mayer, Gierad Laput, and Chris Harrison. 2020. Enhancing mobile voice assistants with worldgaze. In *Proceedings of the 2020 CHI Conference on Human Factors in Computing Systems*. 1–10.

[31] Sven Mayer, Valentin Schwind, Robin Schweigert, and Niels Henze. 2018. The effect of offset correction and cursor on mid-air pointing in real and virtual environments. In *Proceedings of the 2018 CHI Conference on Human Factors in Computing Systems*. 1–13.

[32] Dries Neirynck, Eric Luk, and Michael McLaughlin. 2016. An alternative double-sided two-way ranging method. In *2016 13th workshop on positioning, navigation and communications (WPNC)*. IEEE, 1–4.

[33] Yue Qin, Chun Yu, Wentao Yao, Jiachen Yao, Chen Liang, Yueteng Weng, Yukang Yan, and Yuanchun Shi. 2023. Selecting Real-World Objects via User-Perspective Phone Occlusion. In *Proceedings of the 2023 CHI Conference on Human Factors in Computing Systems*. 1–13.

[34] F Sabath, EL Mokole, and SN Samaddar. 2005. Definition and classification of ultra-wideband signals and devices. *URSI Radio Science Bulletin* 2005, 313 (2005), 12–26.

[35] Jannis Strecker, Khakim Akhunov, Federico Carbone, Kimberly García, Kenan Bektaş, Andres Gomez, Simon Mayer, and Kasim Sinan Yıldırım. 2023. MR Object Identification and Interaction: Fusing Object Situation Information from Heterogeneous Sources. *Proceedings of the ACM on Interactive, Mobile, Wearable and Ubiquitous Technologies* 7, 3 (2023), 1–26.

[36] Scott Sun, Dennis Melamed, and Kris Kitani. 2021. IDOL: Inertial deep orientation-estimation and localization. In *Proceedings of the AAAI Conference on Artificial Intelligence*, Vol. 35. 6128–6137.

[37] Zheng Sun, Aveek Purohit, Raja Bose, and Pei Zhang. 2013. Spartacus: spatially-aware interaction for mobile devices through energy-efficient audio sensing. In *Proceeding of the 11th annual international conference on Mobile systems, applications, and services*. 263–276.

[38] David Verweij, Augusta Esteves, Vassilis-Javed Khan, and Saskia Bakker. 2017. Smart home control using motion matching and smart watches. In *Proceedings of the 2017 ACM International Conference on Interactive Surfaces and Spaces*. 466–468.

[39] Thomas Vincent, Laurence Nigay, and Takeshi Kurata. 2013. Precise pointing techniques for handheld augmented reality. In *Human-Computer Interaction–INTERACT 2013: 14th IFIP TC 13 International Conference, Cape Town, South Africa, September 2–6, 2013, Proceedings, Part I* 14. Springer, 122–139.

[40] Yuntao Wang, Jie Xin Ding, Ishan Chatterjee, Farshid Salemi Parizi, Yuzhou Zhuang, Yukang Yan, Shwetak Patel, and Yuanchun Shi. 2022. FaceOri: Tracking Head Position and Orientation Using Ultrasonic Ranging on Earphones. In *Proceedings of the 2022 CHI Conference on Human Factors in Computing Systems*. 1–12.

[41] Zirui Wang, Shaonian Li, Zhengyuan Zhang, Fan Lv, and Yanzhao Hou. 2018. Research on UWB positioning accuracy in warehouse environment. *Procedia computer science* 131 (2018), 946–951.

[42] Robert Xiao, Gierad Laput, Yang Zhang, and Chris Harrison. 2017. Deus EM Machina: on-touch contextual functionality for smart IoT appliances. In *Proceedings of the 2017 CHI Conference on Human Factors in Computing Systems*. 4000–4008.

- [43] Jun Xu, Maode Ma, and Choi Look Law. 2006. Position estimation using UWB TDOA measurements. In *2006 IEEE International Conference on Ultra-Wideband*. IEEE, 605–610.
- [44] Jing Yang, BaiShun Dong, and Jiliang Wang. 2022. VULoc: Accurate UWB Localization for Countless Targets without Synchronization. *Proceedings of the ACM on Interactive, Mobile, Wearable and Ubiquitous Technologies* 6, 3 (2022), 1–25.
- [45] Fusang Zhang, Zhaoxin Chang, Jie Xiong, Junqi Ma, Jiazhi Ni, Wenbo Zhang, Beihong Jin, and Daqing Zhang. 2023. Embracing Consumer-level UWB-equipped Devices for Fine-grained Wireless Sensing. *Proceedings of the ACM on Interactive, Mobile, Wearable and Ubiquitous Technologies* 6, 4 (2023), 1–27.
- [46] Fusang Zhang, Jie Xiong, Zhaoxin Chang, Junqi Ma, and Daqing Zhang. 2022. Mobi2Sense: empowering wireless sensing with mobility. In *Proceedings of the 28th Annual International Conference on Mobile Computing And Networking*. 268–281.
- [47] Tengxiang Zhang, Zitong Lan, Chenren Xu, Yanrong Li, and Yiqiang Chen. 2023. BLEselect: Gestural IoT Device Selection via Bluetooth Angle of Arrival Estimation from Smart Glasses. *Proceedings of the ACM on Interactive, Mobile, Wearable and Ubiquitous Technologies* 6, 4 (2023), 1–28.
- [48] Tengxiang Zhang, Xin Yi, Ruolin Wang, Jiayuan Gao, Yuntao Wang, Chun Yu, Simin Li, and Yuanchun Shi. 2019. Facilitating Temporal Synchronous Target Selection through User Behavior Modeling. *Proceedings of the ACM on Interactive, Mobile, Wearable and Ubiquitous Technologies* 3, 4 (2019), 1–24.
- [49] Tengxiang Zhang, Xin Yi, Ruolin Wang, Yuntao Wang, Chun Yu, Yiqin Lu, and Yuanchun Shi. 2018. Tap-to-pair: associating wireless devices with synchronous tapping. *Proceedings of the ACM on Interactive, Mobile, Wearable and Ubiquitous Technologies* 2, 4 (2018), 1–21.
- [50] Minghui Zhao, Tyler Chang, Aditya Arun, Roshan Ayyalasomayajula, Chi Zhang, and Dinesh Bharadia. 2021. Uloc: Low-power, scalable and cm-accurate uwb-tag localization and tracking for indoor applications. *Proceedings of the ACM on Interactive, Mobile, Wearable and Ubiquitous Technologies* 5, 3 (2021), 1–31.
- [51] Tianyue Zheng, Zhe Chen, Chao Cai, Jun Luo, and Xu Zhang. 2020. V2iFi: In-vehicle vital sign monitoring via compact RF sensing. *Proceedings of the ACM on Interactive, Mobile, Wearable and Ubiquitous Technologies* 4, 2 (2020), 1–27.
- [52] Zengwei Zheng, Shuang Yan, Lin Sun, Hengxin Shu, and Xiaowei Zhou. 2023. NN-LCS: Neural Network and Linear Coordinate Solver Fusion Method for UWB Localization in Car Keyless Entry System. *Sensors* 23, 5 (2023), 2694.
- [53] Yuan Zhou, Choi Look Law, and Jingjing Xia. 2012. Ultra low-power UWB-RFID system for precise location-aware applications. In *2012 IEEE Wireless Communications and Networking Conference Workshops (WCNCW)*. IEEE, 154–158.